

Comparative Study of Monocrystalline and Polycrystalline Silicon Solar Modules in Kebbi State Environment.

Abubakar Ohinoyi Musa, Adamu Bala Isah

Abstract-The power output of PV modules in general depends on the metrological parameters like irradiance, temperature and humidity applied on each module. However the modules are rated at the standard test conditions (STC) of 1000W/m², AM 1.5 and a module temperature of 25°C, but these conditions do not represent what is typically experienced under outdoor operation. Solar cells with the same efficiency measured in the lab can generate a significantly different amount of electricity when exposed outdoors. For these reasons, there are many regional based studies conducted in the world. This research presents a comparative study of two photovoltaic module technologies conducted under the environmental conditions of Birnin Kebbi, Kebbi State (Nigeria). The study considers monocrystalline (c-Si) and polycrystalline (mc-Si) silicon modules. The I-V characteristics of the modules were measured at regular interval based on the resistive load techniques, during the test period: June, 2018 to October, 2018. The irradiance, ambient and cell temperatures of the modules were also measured. The daily, monthly and the total energy generated over the test period as well as efficiencies and performance ratios were calculated. Performance ratios were found out as 45.50% and 36.70% and the efficiencies as 7.60% and 6.30% for c-Si and mc-Si modules respectively. Total energy generated was 12.10kWh and 10.54kWh in the same order.

Key words: Efficiency (η), Irradiance (G), Monocrystalline (c-Si), Performance Ratio (PR), Polycrystalline (mc-Si), Temperature.

1.0 Introduction

Energy security is one of the most discussed topics today among the readers. For developed nations, the growth of energy consumption is 1% per year, while for developing nations it is around 5% per year. Now in order to maintain the growing energy need there is a need to shift from conventional source of energy to renewable energy, which are sustainable and environment friendly (Siddiqui *et al.*, 2016). The energy demand is increasing worldwide with increasing population and economic development. At present, the energy generation led by conventional energy sources has a severe impact on environmental conditions, energy security due to faster depletion of fossil fuels (Kumar & Kumar 2017). The finiteness of fossil fuels and their effect on climate change has encouraged the search for sustainable energy technologies. One of these technologies is photovoltaics (PV), i.e., solar cell systems for producing electric power (Rode & Weber 2016). Nowadays, photovoltaics (PV) are the most widespread solar energy system worldwide (Almonacid *et al.*, 2016). Among all renewable energy sources, solar energy is gaining extensive interest all around the world, because the sun is the most abundant energy source able to satisfy the energy demand of the whole world (Kumar & Kumar 2017).

Presently PV has become the third most important renewable energy source after hydro and wind

power. By the end of 2014, the terrestrial PV systems installed all over the world had a total capacity of over 150 GW (Ju *et al.*, 2017). Since 2008 there has been a rapid uptake of small-scale solar PV systems on household rooftops. In five years from 2008 to 2013 the number of Australians installing solar photovoltaic (PV) technology grew from 8000 to more than one million (Sommerfeld *et al.*, 2017).

Renewable energy sources are considered as alternative energy sources due to environmental pollution, global warming and depletion of ozone layer caused by green house effect. The Earth receives about 3.8×10^{24} J of solar energy on an average which is 6000 times greater than the world consumption. Solar energy is most readily available source of energy. Solar energy is non-polluting and maintenance free (Shukla *et al.*, 2016). Normal operation of PV modules usually differs from STC, working over a wide range of temperatures, irradiance, and spectra (Polo *et al.*, 2017).

The major share of the solar radiation incident on the PV module does not contribute to produce power. Only 5–20% of the incident solar energy is converted into electricity, depending on the PV cell technology. The remaining energy is converted into heat and affects the current density versus voltage characteristics of the PV module which in turn reduce its electrical power conversion efficiency

(Islam *et al.*, 2016). Photovoltaics is the field of technology and research related to the devices which directly convert sunlight into electricity. The solar cell is the elementary building block of the photovoltaic technology. Solar cells are made of semiconductor materials, such as silicon. One of the properties of semiconductors that makes them most useful is that their conductivity may easily be modified by introducing impurities into their crystal lattice (Commission 2009).

The most established solar PV technologies are silicon based systems (Ellabban *et al.*, 2014). Almost all solar cells that have been previously used in the terrestrial and space missions have been the p-n junction silicon variety (Musa 2010). Silicon solar cells containing boron and oxygen are one of the most rapidly growing forms of electricity generation. However, they suffer from significant degradation during the initial stages of use. This problem has been studied for 40 years resulting in over 250 research publications (Contreras *et al.*, 2019).

PR is an indicator of losses resulting from inverter problems, wiring, shading, cell mismatch, reflection, outages, module temperatures etc The temperature of the study environment affects the PR of the modules etc. (Khalid *et al.*, 2016). In designing any power generation system that incorporates photovoltaics (PV) there is a basic requirement to accurately estimate the output from the proposed PV array under operating conditions. PV modules are given a power rating at standard test conditions (STC) of 1000Wm^{-2} , AM1.5 and a module temperature of 25°C , but these conditions do not represent what is typically experienced under outdoor operation (Carr & Pryor 2004). Several studies have focused on the knowledge, for a given natural environment, of the photovoltaic technology that provides the best trade-off between the cost and the performances of the module (Tossa *et al.*, 2016).

This study is thus aimed at the comparative study of both types of silicon solar modules to determine which will be best suited for use in the generally hot environment of Kebbi State, Nigeria.

1.1 Study Location

Birnin-Kebbi is the capital of Kebbi State in North Western Nigeria. It falls within Latitude 12.4539°N and Longitude 4.1975°E of the equator. Birnin-Kebbi is a tropical region with an average temperature of 32°C . It is characterized by seasonal rainfall which usually commence in April and last to October, though with heavy rainfall in

July and August (Ogunbajo *et al.*, 2015).

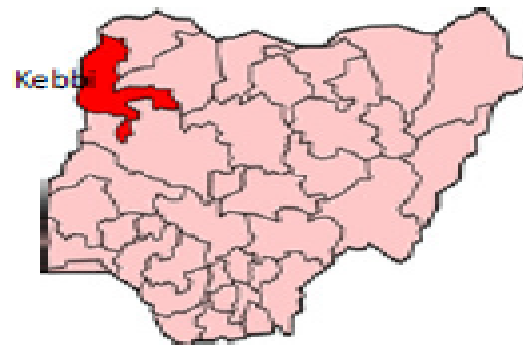


Fig 1. Map of Nigeria showing Kebbi State (Ismail & Oke 2012).

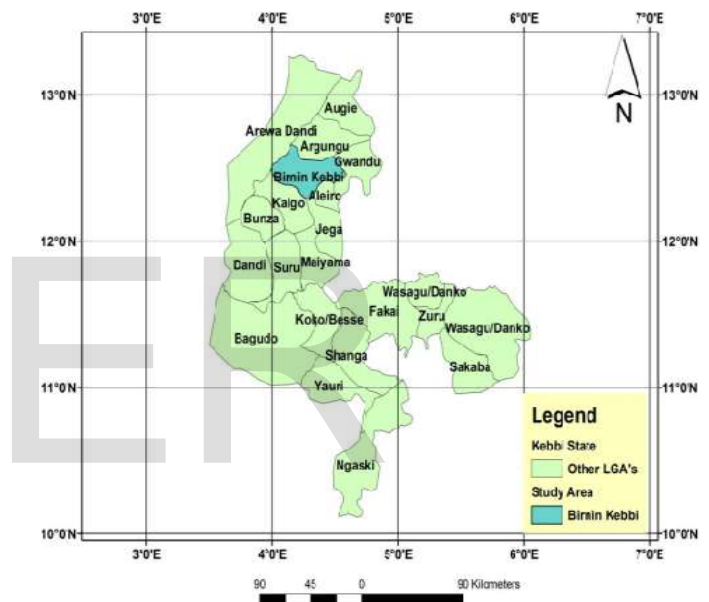


Fig. 2. Map of Kebbi State showing Birnin Kebbi (Ogunbajo *et al.*, 2015).

2.0 Review of Previous Works

Several studies have focused on the knowledge, for a given natural environment, of the photovoltaic technology that provides the best trade-off between the cost and the performances of the module (Tossa *et al.*, 2016).

Balaska *et al.*, (2017) carried out the performance assessment of five different photovoltaic module technologies under outdoor conditions in Algeria: copper indium selenide (CIS), monocrystalline heterojunction with intrinsic thin layer (HIT), tandem structure of amorphous silicon and microcrystalline silicon (a-Si $_{\mu\text{c}}$ -Si), multi-crystalline and mono-crystalline back contact. It was found that the HIT and the a-Si $_{\mu\text{c}}$ -Si performed much better than the other technologies.

Elibol *et al.*, (2017) analyzed different PV panel types: monocrystalline, polycrystalline and amorphous silicon at Düzce University Scientific and Technological Research Application and Research Centre (DUBİT) in Düzce Province, in Turkey. Performance ratios were found out as 73%, 81% and 91% for a-Si, polycrystalline and monocrystalline PV panels, respectively. Panel efficiency was calculated as 4.79%, 11.36% and 13.26% in the same order.

Siddiqi *et al.*, (2016) compared five different technologies for solar PV (Photovoltaic) outdoor performance using indoor accelerated aging tests for long term reliability: Mono, Multi, a-Si, CdTe and CIGS. The study established the performance dominance of c-Si (Mono) technology over all the thin film technologies based on stress tests and evaluation through the repeated measurement of maximum Power, module efficiency and cell efficiency.

Tossa *et al.*, (2016) studied the performance comparison of four photovoltaic technologies under hot and harsh climate of Ouagadougou, Burkina Faso. The modules includes: one monocrystalline (c-Si), two polycrystalline (p-Si) from different manufacturers and one tandem structure of amorphous/microcrystalline (a-Si/ μ c-Si). The results showed that the micromorphous module presents the best performance on the selected site, with an average performance ratio of 92%.

Bianchini *et al.*, (2016) revealed the performance analysis and economic assessment of different photovoltaic technologies based on experimental measurements at HEnergia located in the industrial area of Forli, Italy. The study analyzed Heterojunction with Intrinsic Thin layer (HIT), polycrystalline (poli c-Si), cadmium telluride (CdTe), amorphous silicon with microcrystalline silicon (a-Si/ μ c-Si), and triple-junction III-V gallium arsenide cells (GaAs). The study showed that poli-Si with solar tracking system was characterized by the highest energy production for each month and if only the fixed installations are considered, the energy yields were quite similar in the autumn and winter periods, while in the summer time the performance of thin film technologies, i.e. (CdTe) and (a-Si/ μ c-Si), is higher than HIT and poli c-Si.

Aste *et al.*, (2014) carried out performance comparison of three different PV technologies in temperate climates. The tested technologies are: crystalline silicon cells (c-Si), micromorphous cells (a-Si/ μ c-Si) and heterojunction with intrinsic thin layer (HIT) cells. According to the study the average annual PR of the three technologies is quite similar, with a maximum value for HIT technology (96%), and lower values for the c-Si (93%) and a-Si/ μ c-Si modules (91%). However, in

warmer months micromorphous a-Si/ μ c-Si silicon cells, in fact, achieve a performance higher than the other technologies tested.

Başoğlu *et al.*, (2015) analyzed the performance of different photovoltaic module technologies under İzmit, Kocaeli climatic conditions, Turkey. The analyzed modules are: crystalline (c-Si), multicrystalline (mc-Si) and cadmium-telluride (CdTe) modules. The study accepted CdTe as more reliable array under İzmit climatic condition and the mean values of PRs are 83.8%, 82.05% and 89.76% for mc-Si, c-Si and CdTe arrays, respectively.

Carr & Pryor (2004) compared the performance of different PV module types in temperate climate of Perth, Western Australia. The modules examined in this study are: crystalline silicon (c-Si), laser grooved buried contact (LGBC) c-Si, polycrystalline silicon (p-Si), triple junction amorphous silicon (3j a-Si) and copper indium diselenide (CIS). The superior module in this analysis is the LGBC c-Si module BP585, with efficiency values between 11.5% and 12.5%.

Peters *et al.*, (2018) found that materials with smaller band gaps are generally more sensitive to temperature and precipitable water, and perform relatively better in cold and dry locations, e.g., mountain ranges and temperate climates (northern North America, northern Asia, and high mountain ranges including the Andes and Himalayas). Materials with larger band gaps perform relatively better in hot and humid locations, e.g., tropics and subtropics (South America, Africa, the Arabian Peninsula, India, South and Southeast Asia, the southern United States, and parts of China). Similar performance for different technologies is found in temperate regions in Europe, central Asia, central United States, and Japan.

2.1 Theoretical Background

The direct conversion of sunlight to electricity is likely to be a prime energy source for the future assuming that the practical economic means of direct conversion can be developed. Photovoltaic modules can provide an independent, reliable electrical power source at point of use making it particularly suited for remote or inaccessible locations (Musa 2010). Solar PV technology is the most significant renewable energy technology particular for remote and stand-alone consumers away from main electrical distribution network (Rao & Parulekar, 2007).

2.1.1 The Photovoltaics

The term “photovoltaic” refers to a family of technologies that convert light directly into electricity (Harmon, 2000). Photovoltaic

technologies have been highlighted as an ideal source of energy due to its non-polluting performance in the way it produces electricity by harvesting the energy available from the Sun, which is a free source of energy (Espinosa *et al.*, 2017). One of the most sustainable and economically competitive renewable energy sources is solar photovoltaic (PV) energy. Moreover, solar PV energy increases a country's energy security by reducing dependence on fossil fuels (Garoudja *et al.*, 2017).

2.1.2 PV Cell Technology

Solar cells can be categorized into two main groups: wafer type (single crystalline or multi-crystalline) and thin film (a-Si, Cd-Te and CIGS). The former are made from wafers cut from a silicon ingot, and the latter are made by depositing silicon directly onto a substrate such as glass or steel. Wafer-type solar cells dominated 95% of commercial PV market while the remaining 5% were mainly PV silicon thin-film solar cells in 2007 (Waheed *et al.*, 2012). The various types of materials applied for photovoltaic solar cells includes mainly in the form of silicon (single crystal, multi-crystalline, amorphous silicon) cadmium-telluride, copper-indium-gallium-selenide, and copper-indium-gallium-sulfide.

On the basis of these materials, the photovoltaic solar cells are categorized into various classes as also shown in below (Sharma *et al.*, 2015).

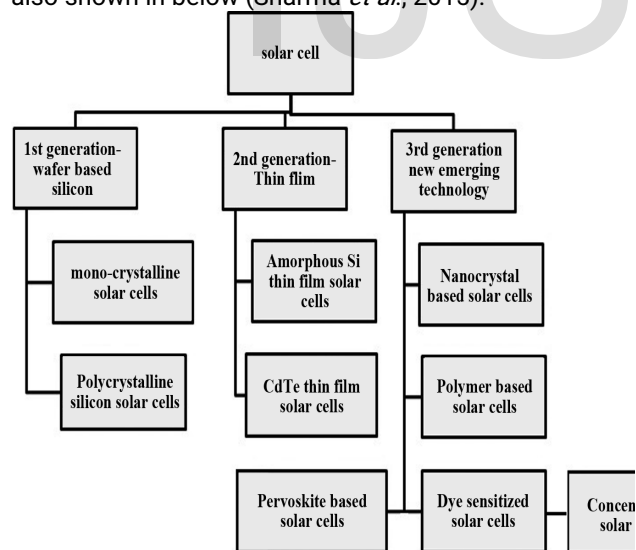


Fig 3. various types of solar cell technologies and current trends of development (Sharma *et al.*, 2015)

2.1.2(a) Monocrystalline Si Solar cell

Monocrystalline silicon, also known as called single crystalline silicon, is a crystalline solid, in which the crystal lattice is continuous and unbroken without any grain boundaries over the entire bulk, up to the edges (Jager *et al.*, 2014). The efficiency of mono-crystalline single-crystalline

silicon solar cells lies between 17% - 18% (Sharma *et al.*, 2015)

2.1.2(b) Polycrystalline Si Solar cell

While a monocrystalline silicon wafer has one uniform color, in multicrystalline silicon, the various grains are clearly visible for the human eye. The more grain boundaries in the material, the shorter the lifetime of the charge carriers. Hence, the grain size plays an important role in the recombination rate (Jager *et al.*, 2014). Though they are slightly cheaper to fabricate compared to monocrystalline silicon solar panels, yet are less efficient ~12% - 14% (Sharma *et al.*, 2015).

2.1.3 Solar cell parameters and equivalent circuit

(a) The main parameters that are used to characterize the performance of solar cells are the peak power P_{max} , the short-circuit current density J_{sc} , the open-circuit voltage V_{oc} , and the fill factor FF. These parameters are determined from the illuminated J-V characteristic. The conversion efficiency η can be determined from these parameters (Jager *et al.*, 2014). These four quantities J_{sc} , V_{oc} , FF and η define the performance of a solar cell, and are thus its key characteristics (Pagliaro *et al.*, 2008).

(i) The short-circuit current (I_{sc})

The short-circuit current I_{sc} is one of the most essential characteristics of a solar cell. It occurs in an illuminated, short-circuited solar cell (Krauter, 2006). Ideally this is equal to light-generated current I_L (Green, 1982).

$$I = I_L - I_0 \left[\exp\left(\frac{q(V + IR_s)}{AkT}\right) - 1 \right] - \frac{V + IR_s}{R_{sh}} \quad (1)$$

where I_d is the junction current of the diode

$$I_d = I_0 \left[\exp\left(\frac{q(V + IR_s)}{AkT}\right) - 1 \right] \quad (2)$$

I , the load current

I_L , the photovoltaic current,

I_0 , the reverse saturation current

q , electronic charge,

k , boltzmann constant,

T , absolute temperature, A , factor of the diode quality

R_s , series resistance,

R_{sh} , parallel resistance (Grid 2010).

(ii) The open-circuit voltage (V_{oc})

The voltage V_{oc} developed when the terminals are isolated is the open circuit voltage (Pagliaro *et al.*, 2008)

$$V_{oc} = \frac{kT}{q} \ln\left(\frac{I_L}{I_0} + 1\right) \approx \frac{kT}{q} \ln\left(\frac{I_L}{I_0}\right) \quad (3)$$

(Grid 2010)

(iii) The fill factor

Fill factor is another important parameter which tells about quality of cell/module and its value

should lie between 0.7–0.8 as per IEC standard (Berwal *et al.*, 2017). It is defined as the ratio of maximum power to the product of open circuit voltage and short circuit current. This factor is obtained by comparing the maximum power to the theoretical power (Mathew *et al.*, 2018). The fill factor FF is thus defined as the ratio

$$FF = \frac{J_m V_m}{J_{sc} V_{oc}} \quad (4)$$

(Berwal *et al.*, 2017).

The FF thus describes the squareness of the J–V curve (Pagliaro *et al.*, 2008)

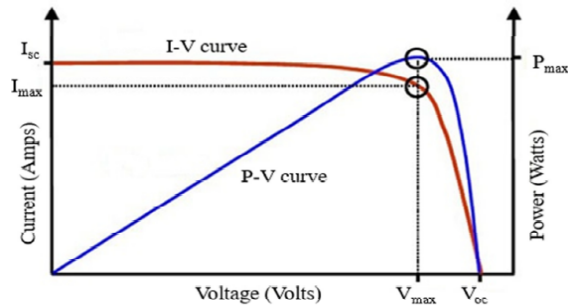


Fig 4. I-V and P-V curves (Mathew *et al.*, 2018)

(iv) The electrical power conversion efficiency

The photovoltaic conversion efficiency η is defined by the ratio of the PV electrical power output to the irradiated power on a solar cell. The conversion efficiency is determined under standard test conditions (STC) (Krauter, 2006). The solar cell power conversion efficiency can be given as:

$$\eta = \frac{P_{max}}{P_{in}} = \frac{I_{max} \times V_{max}}{I(t) \times A} \quad (5)$$

Where I_{max} and V_{max} are the current and voltage for maximum power, corresponding to solar intensity $I(t)$ and A is Area of solar cell (Fesharaki *et al.*, 2011).

When the PV modules work in a real environment, the measured DC power (W), P_{DC} , can be very different from the nominal one due to variation in module temperature T_c ($^{\circ}C$) and/or irradiance G (W/m^2). The DC efficiency η_{DC} of PV modules can be defined as the ratio between measured DC power P_{DC} and the product of surface area of modules A with the measured irradiance G .

$$\eta_{dc} = \frac{P_{dc}}{A \times G} \quad (6)$$

PV efficiency can be calculated in instant, hourly,daily,monthly and yearly periods. Hourly efficiency is expressed as

$$\eta_{sys,h} = \frac{E_{sys,h}}{S.Gopt,h} \quad (7)$$

(Elibol *et al.*, 2017)

$E_{sys,h}$,shows hourly AC power amount transferred to power plant by the system, S total surface area of the panels and $Gopt,h$ hourly radiation energy reflecting onto unit area of panel surface. Daily efficiency analysis can be expressed with

$$\eta_{sys,d} = \frac{E_{sys,d}}{S.Gopt,d} \quad (8)$$

(Elibol *et al.*, 2017)

$E_{sys,h}$,represents daily AC energy amount transferred to power plant by the system (kW h) and $Gopt,h$,daily amount of radiation reflecting onto unit area of panel surface (kWh/m²). Average system efficiency per month can be expressed with

$$\eta_{sys,m} = \frac{\sum_{i=1}^n (E_{sys,d})_i}{\sum_{i=1}^n (Gopt,d)_i} \quad (9)$$

(Elibol *et al.*, 2017).

(b) A solar cell is a non-linear device and can be represented as a current source model as shown in figure 1.4. The current source I_{ph} represents the cell photo current, I_d is reverse saturation current of diode, R_{sh} and R_s are the intrinsic shunt and series resistance of the cell respectively. Usually the value of R_{sh} is very large and that of R_s is very small, hence they may be neglected to simplify the analysis (Singh, 2013).

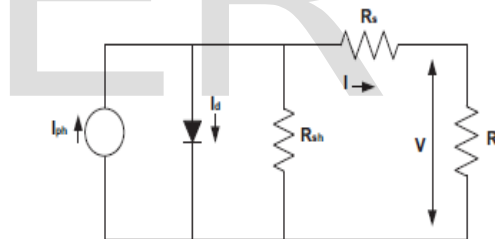


Fig 5. Simplified equivalent circuit of a photovoltaic cell (Singh, 2013).

2.1.4 Current-Voltage (I-V) characteristics of a solar cell.

The typical I-V characteristic of a PV array is given by the following equation

$$I = N_p I_{pn} - N_p I_d \left[\exp\left(\frac{qV}{kTAN_s}\right) - 1 \right] \quad (10)$$

where, I is the PV array output current (A), V is the PV array output voltage (V), N_s is the number of cells connected in series, N_p is the number of modules connected in parallel, q is the charge of an electron, k is the boltzman’s constant, A is the pn junction ideality factor, I_d is the cell reverse saturation current, T is the cell temperature. The factor ‘ A ’ determines the cell deviation from the ideal pn junction characteristic; it ranges from 1 to

5, 1 being the ideal value.

The cell reverse saturation current I_d varies with temperature according to the following equation

$$I_d = I_c [T/T_c]^3 \exp\left[\left(\frac{E_g}{kTN_s}\right)\left(\frac{1}{T_c} - \frac{1}{T}\right)\right] \quad (11)$$

where, T_c is the cell reference temperature, I_c is the reverse saturation current at T_c , and E_g is the band gap energy of the semiconductor used in the cell. The photo current I_{ph} depends on the solar radiation and the cell temperature as given by:

$$I_{ph} = [I_{sc} + K_i(T - T_c)] [S/100] \quad (12)$$

where, I_{sc} is the cell short circuit current at reference temperature and radiation, K_i is the short circuit current temperature coefficient, and S is the solar radiation in mW/cm^2 (Singh, 2013).

2.1.5 Performance Ratio (PR)

The PR represents the actual energy generated by the PV plant to its expected energy with reference to its name plate rating. In other words, the PR is an indicator of losses resulting from inverter problems, wiring, shading, cell mismatch, reflection, outages, module temperatures etc (Khalid *et al.*, 2016). The PR calculated using the maximum power values measured outdoor is a better indicator of the technology's performance, when several PV modules are compared. It is a dimensionless quantity normalized with respect to the incident solar radiation. It is given

$$PR = \frac{\eta}{\eta_{STC}} \quad (13)$$

where η and η_{STC} are the module efficiencies under real operating conditions and standard test conditions respectively, with the efficiencies calculated as

$$\eta = \frac{P_{max}}{A \times G} \times 100\% \quad (14)$$

$$\eta_{STC} = \frac{P_{max,STC}}{A \times G_{STC}} \times 100\% \quad (15)$$

where A represents the active area of the module (m^2); G the solar irradiance (W/m^2); and P_{max} the maximum power of the module (Tossa *et al.*, 2016). The PR index measures the deviation between the actual performance of a PV system and that theoretically achievable under standard test conditions (STC) and it may be defined as:

$$PR = \frac{E \times I_{stc}}{H \times P} \quad (16)$$

where E ($W h$) is the output energy generated by the module in the selected time period, I_{stc} is the solar irradiance under standard test conditions, H is the solar irradiation on the module plane in the selected time ($W h/m^2$) and P (W) is the nominal power of the module measured under standard test conditions (Aste *et al.*, 2014).

2.1.5 Factors Affecting PV Performance

Solar irradiance and cell temperature are two factors, which affect the performance of a PV module (Reza *et al.*, 2016). The performance of solar PV modules is highly dependent on meteorological conditions (Balaska *et al.*, 2017). The output power from the PV module is dependent on the solar irradiance and ambient temperature of the site:

$$P_{pv} V(s) = N \times FF \times V_y \times I_y \quad (17)$$

Where N is the number of modules and FF is the fill factor given as:

$$FF = \frac{V_{mpp} \times I_{mpp}}{V_{oc} \times I_{sc}} \quad (18)$$

In which V_{oc} and I_{sc} are the open circuit voltage and short circuit current of the module and V_{mpp} and I_{mpp} are the voltage and current corresponding to the maximum power point.

Also

$$V_y = V_{oc} - K_v \times T_c \quad (19)$$

and

$$I_y = s [I_{sc} + K_i \times (T_{cy} - 25)] \quad (20)$$

$$T_{cy} = T_a + s \left(\frac{Not - 20}{0.8} \right) \quad (21)$$

Where T_{cy} and T_a are cell and ambient temperatures respectively, K_i and K_v are current and voltages temperatures coefficients respectively, Not is the nominal operating temperature of a cell (Guwaeder & Ramakumar 2017).

It is found that PV performance falls with the increase in module temperature. The efficiency of crystalline silicon solar cells fall by 0.5% for every 1 °C rise in solar cell temperature and this decrease in efficiency varies with the type of cell (Chandel & Agarwal 2017). The high temperature of PV cell has adverse effect on the performance of PV cell. The increase in temperature of PV cell causes, 0.06–0.1%/°C rise in its short circuit current, but; power output, fill factor and open circuit voltage decreased to 0.4–0.5%/°C, 0.1–0.2%/°C and 2–2.3 mV/°C respectively (Sathe & Dhoble 2017). For the same irradiance level, the output power and therefore the efficiency decreases with increased cell temperature. The efficiency depends strongly on the temperature of the PV module and an overheating causes a decrease in the produced energy (Zaoui *et al.*, 2015).

3.0 Materials and Methods

The list and details of materials used and the method employed in this study are presented in this part.

3.1 List and Details of Used Materials

The materials used in this work are: Monocrystalline module (c-Si), Polycrystalline

module (mc-Si), Four Digital Multimeters, Three Rheostats, Thermocouple Thermometer, Connecting Wires, Light Source (Sunlight) and DC Regulated Power Supply.

The details of tested modules and data-monitoring system are described in Table 1 & 2. The modules parameter were given under Standard Test Condition (STC): Air mass (AM) =1.5, Irradiance (G_{stc}) =1000Wm² and Cell temperature (T_c) =25°C.

Table 1. Details of the monitoring equipment.

Equipment	Digital multimetres	DC regulated power supply	Rheostat
Model	DT9205A	305D	
Range	DC(200mV-1000V) DC(2mA-20A)	0-30V 0-5A	1A, 0-100Ω 1A, 0-180Ω 1.7A, 0-265Ω
Accuracy	±(0.5%+1dgt)		
Precision		±1%	

Table 2(a). Electrical specifications of the modules at STC.

Module technology	c-Si	mc-Si
Module manufacturer	Sunshine Solar	Sunshine Solar
Maximum Power(Pmax)[W]	80W	80W
Current at Pmax(Imp)[A]	4.57A	4.57A

Voltage at Pmax(Vmp)[V]	17.5V	17.5V
Short-circuit current(Isc)[A]	5.12A	5.12A
Open-circuit voltage(Voc)[V]	22.05V	22.05V
Module efficiency at STC(η)[%]	17%	12.9%
Weight[Kg]	8kg	5.68kg
Output tolerance	±5%	±5%
Active area(A)[m ²]	0.58 m ²	0.50m ²

Table 2(b). Details of the data-monitoring equipment.

Sensor box	
Solar irradiation sensor	Solar power meter(TM-206)
Measurement range	0-2000W/m ²
Accuracy	±5%
Resolution	0.1W/m ²
Temperature sensor	TM-902C K type thermometer with probe
Measuring sensor	Thermocouple sensor probe
Measurement range of TM-902C	-50°C-1300°C
Measurement range of TP-02A probe	-50°C-700°C
Accuracy	<400°C ± 0.75%

3.2 Methods

Two different PV modules, were installed at Bayan Tasha, Birnin Kebbi, Kebbi State (Latitude 12.4539°N, Longitude 4.1975°E). The modules were south-exposed, mounted on a fixed support on the ground and tilted at angle of 27°. The tilt angle of the PV module is correlated with the location latitude angle and the season. The modules under test in this study were: Monocrystalline (c-Si) and Polycrystalline (mc-Si) with an active areas of 114.0cm×50.6cm and 104.8cm×47.5cm respectively, and were monitored from June, 2018 to October, 2018.

3.2.1 I-V and P-V Characteristic Measurement

Both modules were connected to an I-V curve system based on resistive load technique. Variable resistors (rheostats) considered as load resistors were used, the step variation of these resistors implies the variations of the values of currents (I_m) and voltages (V_m). In one of the I-V systems, two rheostats: that of 0-100Ω and that of 0-180 Ω were connected in series to form a net of 280 Ω resistance while the other system has a rheostat of resistance 0-265 Ω.

With the help of multimeters, the modules parameters: short circuit current (I_{sc}), the open circuit voltage (V_{oc}), module current (I_m) and voltage (V_m) values with variation of load achieved through rheostats were all measured. Each time, the value of current for zero voltage and the value of voltage for zero current were taken first and these correspond to short-circuit current (I_{sc}) and open-circuit voltage (V_{oc}) respectively. Then the current and voltage values taken with variation in the load achieved through the rheostat. The I-V data were obtained from multiple measurement each day, at different weather conditions. The measurement was conducted on hourly interval each day (from 10:00AM to 4:00PM) and readings were taken within 10-15 minutes so short that the solar radiation can be considered constant for all the points.

Finally the dark characteristics of modules were measured using an external DC power supply in forward bias mode and the panels kept in dark condition. The supply voltage was increased in steps and the currents measured.

3.2.2 Measurement of Temperature and Irradiance

The thermocouple thermometer was in the measurement of ambient temperature (T_a) and the cell temperature (T_c) of the modules in °C. The

solar power meter was employed in measuring the solar irradiance (G) in Wm^{-2} . The experimental layout and set-up were shown in Fig 9 and 10.

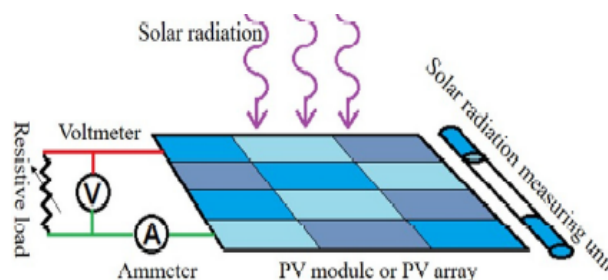


Fig 6. Experimental layout (Mathew *et al.*, 2018)

The measured temperatures and irradiance obtained during measurement interval were summed up to get the total daily and their corresponding average values. They were all plotted on graph together with modules' parameters: efficiencies performance ratios, V_{oc} , and I_{sc} over the test period so as observe their relations. Their various correlation coefficients were also calculated in order to determine the strength of these relations. All calculations were carried out in excel spread sheets.

The measured data were all recorded and entered in excel spread sheet. With the monitored data: V_{oc} , I_{sc} , I_m , V_m , G, T_a and T_c , the I-V and P-V curves were plotted, maximum power (P_{max}), fill factor, daily energy generated, hourly efficiency, daily efficiency, monthly efficiency and daily performance ratio (PR) were all calculated

3.2.3 Calculation of Power Rating for a Specified Period of Time

The electrical power generated was calculated by multiplying current and voltage values. From the power values calculated, the maximum powers were sorted out and were also identified on the P-V characteristic curve. The produced for a given day is computed in accordance with the work of Balaska *et al.*, (2017), for each day, the energy produced by each module is calculated as follows:

$$E = \tau \sum P_{mea} \quad (22)$$

where

E is expressed in Wh;

P_{mea} is the measured maximum power in W;

τ is the recording time interval.

That is the summation of maximum powers across the recording time interval gives the total energy generated over that time. The daily, monthly and the total energy generated over the monitoring were calculated.

3.2.4 Calculation of Electrical Power Conversion Efficiency (η)

The calculation of the electrical power conversion efficiency is essential so as to study how metrological conditions affect it. The hourly, daily and monthly efficiencies were calculated using equation (7), (8) and (9) respectively.

3.2.5 Performance Ratio (PR) Calculation

The PV technologies were analyzed and compared in terms of performance ratio (PR) on energy. The PR index measures the deviation between the actual performance of a PV system and that of theoretically achievable under Standard Test Conditions (STC). The performance ratios were calculated using equation (16).

4.0 Results and Discussion

In this part, the data produced between 13 June 2018 and 31 October 2018 by the two types of PV systems mounted at Bayan Tasha, Birnin Kebbi is explained in details. There are 140 days over the monitoring period. However, starting from that date, some data are missing due to the external events, such as rainfall, breakdown of measuring devices, incomplete date acquisition for a given day. As a result, there are 90 total days with comparable data across the monitoring. The missing days were ignored in the calculations of performance indexes, and this is in accordance with the literature.

Khalid *et al.*, (2016) highlighted that, if there is problem due to plant availability, say inverter was not operational for two days in a month then one should ignore these two days for PR calculation. Bianchini *et al.*, (2016) monitored PV data from 1st June 2013 to 28th October 2014, that is, 515 days of measurements, however, 285 days were recorded, due to some external events.

4.1 Result of Current-Voltage (I-V) and Power-Voltage (P-V) Characteristics

The detailed comparison of the modules is presented with respect to parameters like P_{max} , η , T_c , I_{sc} , V_{oc} , FF, PR etc. The I-V and P-V characteristics of the modules for some sample clear days are shown in figure 7-12 below.

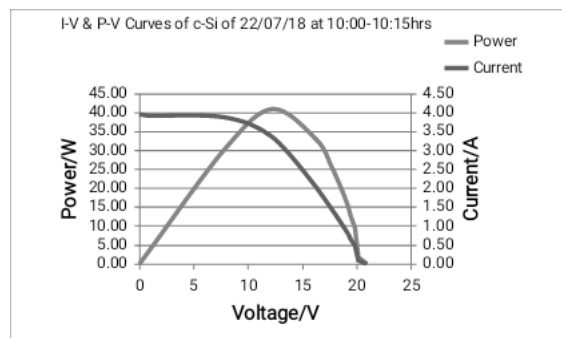


Figure 7. I-V and P-V curves of c-Si module, on 22/07/18 at 10:00-15am, $G=775W/m^2$, $T_a=32.9^\circ C$, $T_c=39.5^\circ C$, $\eta=9.17\%$, $FF=0.50$, $PR=57.51\%$.

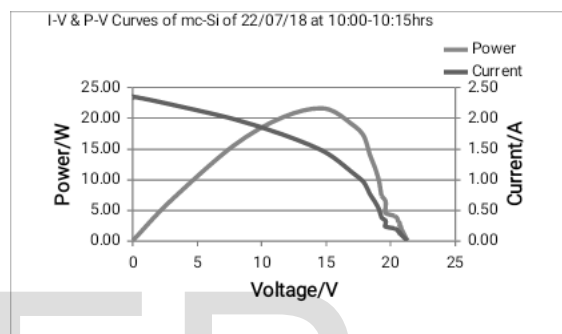


Fig 8. I-V and P-V curves of mc-Si module, on 22/07/18 at 10:00-15am, $G=780W/m^2$, $T_a=32.9^\circ C$, $T_c=40.1^\circ C$, $\eta=5.56\%$, $FF=0.43$, $PR=38.79\%$.

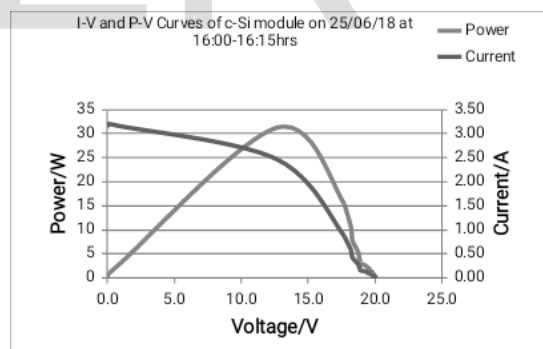


Fig 9. I-V and P-V curves of c-Si module, on 25/06/18 at 4:00-4:15pm, $G=405W/m^2$, $T_a=36.5^\circ C$, $T_c=48.1^\circ C$, $\eta=13.37\%$, $FF=0.49$, $PR=54.50\%$.

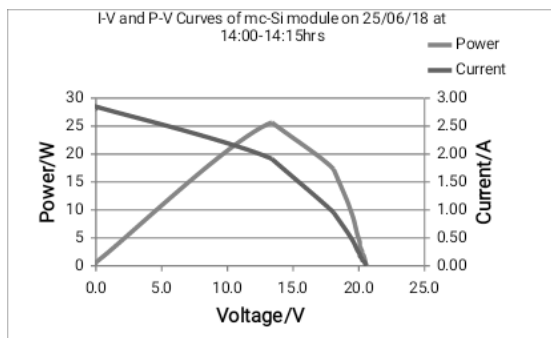


Fig 10. I-V and P-V curves of mc-Si module on 25/06/18 at 2:00-2:15pm, $G=757W/m^2$, $T_a=36.8^\circ C$, $T_c=51.2^\circ C$, $\eta=6.83\%$, $FF=0.44$, $PR=39.22\%$.

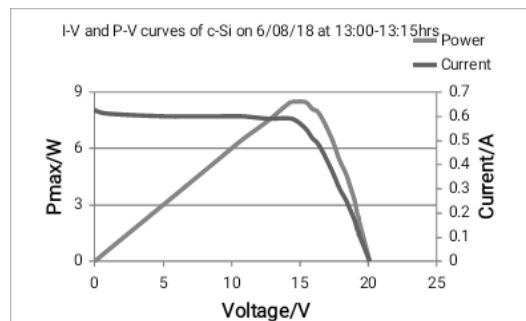


Fig 13. I-V and P-V curves of c-Si module, on 6/08/18 at 13:00-15pm, $G=75W/m^2$, $T_a=25.7^\circ C$, $T_c=27.7^\circ C$, $\eta=19.64\%$, $FF=0.67$, $PR=107.06\%$.

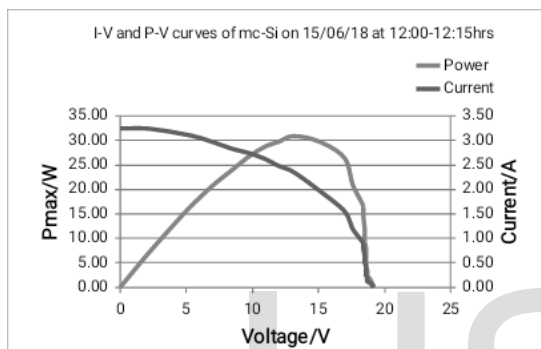


Fig 11. I-V and P-V curves of mc-Si module, on 15/06/18 at 12:00-12:15pm, $G=940W/m^2$, $T_a=40.5^\circ C$, $T_c=61.7^\circ C$, $\eta=6.61\%$, $FF=0.5$, $PR=36.96\%$.

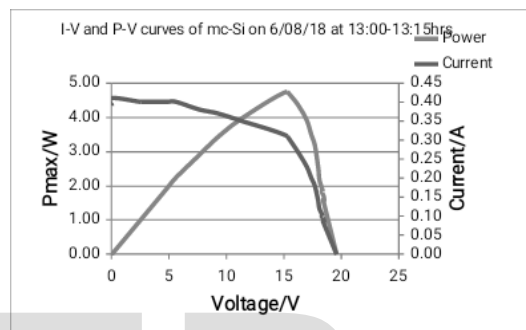


Fig 14. I-V and P-V curves of mc-Si module, on 6/08/18 at 13:00-13:15pm, $G=93W/m^2$, $T_a=25.7^\circ C$, $T_c=28.0^\circ C$, $\eta=10.25\%$, $FF=0.62$, $PR=62.28\%$.

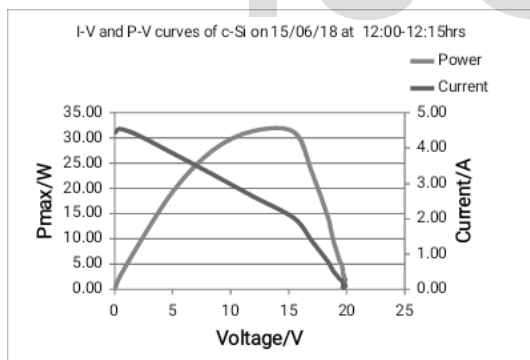


Fig 12. I-V and P-V curves of c-Si module, on 15/06/18 at 12:00-12:15pm, $G=933W/m^2$, $T_a=40.5^\circ C$, $T_c=63.3^\circ C$, $\eta=5.84\%$, $FF=0.36$, $PR=54.7\%$.

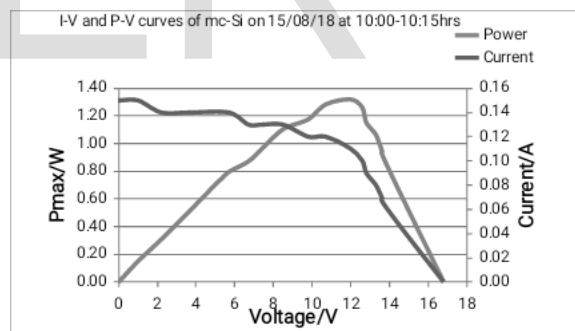


Fig 15. I-V and P-V curves of mc-Si module, on 15/08/18 at 10:00-15pm, $G=28W/m^2$, $T_a=27.8^\circ C$, $T_c=29.0^\circ C$, $\eta=9.47\%$, $FF=0.52$, $PR=46.96\%$.

Some samples of the modules' I-V and P-V characteristics in overcast days are also shown in fig 13-16 below.

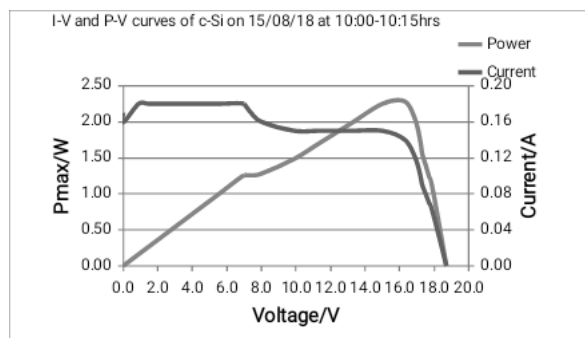


Fig 16. I-V and P-V curves of c-Si module, on 15/08/18 at 10:00-15pm, $G=20.0\text{W/m}^2$, $T_a=27.8^\circ\text{C}$, $T_c=28.6^\circ\text{C}$, $\eta=19.78\%$, $FF=0.72$, $PR=37.26\%$.

Also the dark characteristics of the two modules are shown in fig 17.

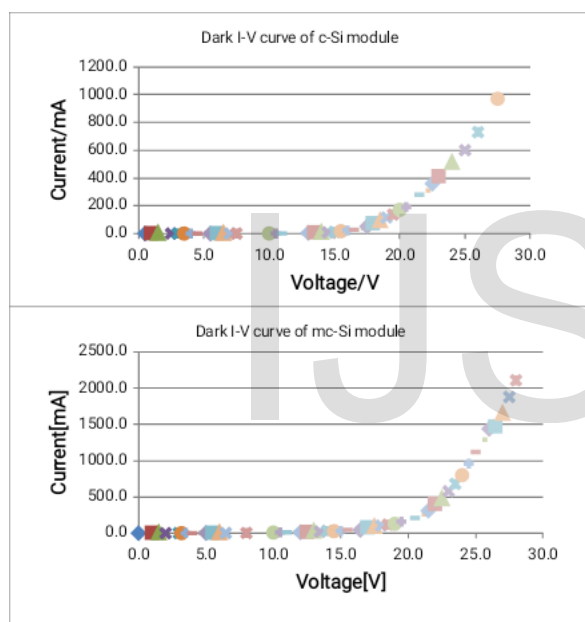


Fig 17. Dark I-V characteristics of the monocrystalline (c-Si) and polycrystalline (mc-Si) modules.

4.2 Result of The Effect of Temperature and Solar Irradiance on the Modules' Parameters

The daily analysis is useful, because the incident spectrum can shift significantly toward the red or the blue, both in the course of the day and seasonally (Aste *et al.*, 2014). This work is aimed at the measurement of outdoor performances of the modules, hence it is fundamental to analyze the real operating conditions recorded during test period on the site.

4.2.1 Temperature and Solar Irradiance of Study Location Over the Test Period

Fig 18 shows the daily average irradiance and ambient temperature observed during the monitoring period. The irradiance and temperature were found to be positively correlated with a calculated pearson correlation of ($r = 0.93$) and ($r = 0.92$) for c-Si and mc-Si modules respectively. The minimum and the maximum recorded average daily irradiance were 60.7W/m^2 in August and 803.1W/m^2 in July, while 26.2°C in August and 41.5°C in June for ambient temperature.

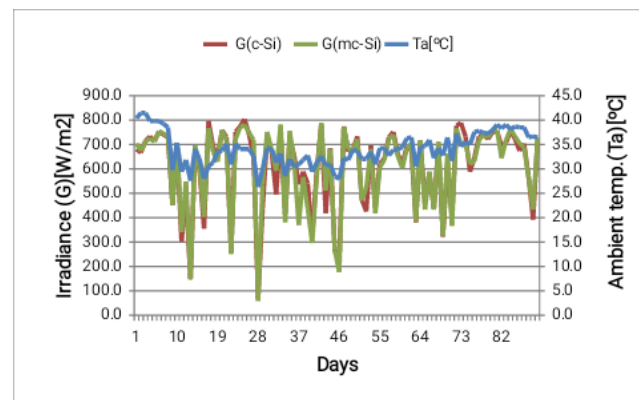


Figure 18. Daily average irradiance (G) and daily average ambient temperature (Ta) over the test period.

Fig 19 shows the module temperatures and the ambient temperature, and both were found have to a positive correlation. The two cell temperatures have correlation coefficients of ($r=0.99$), and for the cell temperatures and ambient temperature the values were ($r=0.93$) and ($r=0.92$) for the monocrystalline and polycrystalline panels respectively. These agree with the findings of elibol *et al.*, (2017). The observed minimum and the maximum average daily cell temperature values were 28.0°C in August and 62.4°C in June.

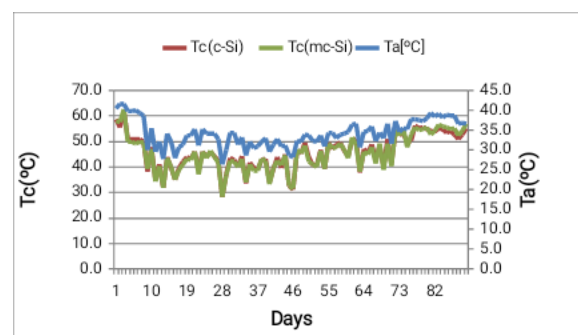


Fig 19. Daily average ambient temperature (Ta) and cell temperature (Tc) over the monitoring period.

Fig 20 shows the monthly average daily irradiation and the module temperature.

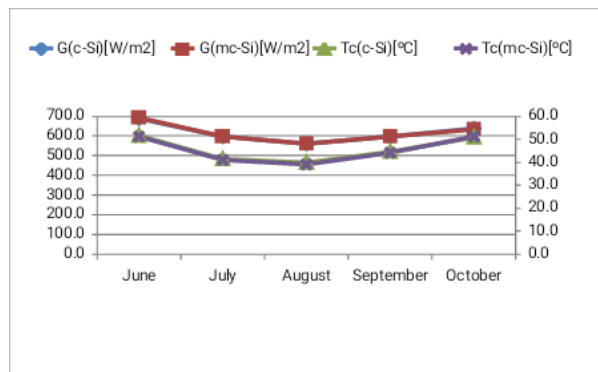


Fig 20. Monthly average daily irradiations and cell temperatures of the modules.

The monthly average daily cell temperatures are determined in range of 51.5°C- 39.6°C, with an average of 45.4°C for c-Si and 51.1°C -39.1°C, with an average of 45.1°C for mc-Si. The average daily irradiation is found in the range of 668.7W/m²-560.4 W/m², with an average of 614.8 W/m² for c-Si and for mc-Si as 692.0W/m²-557.1W/m², with an average of 615.1W/m² respectively.

4.2.2 Effect of Temperature on the Modules' Efficiencies and Performance Ratios

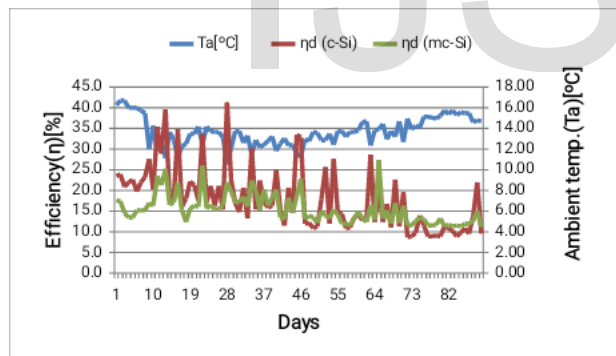


Fig 21. Daily average efficiency (ηd) and ambient temperature (Ta) over the monitoring period.

The daily efficiencies and the average daily ambient temperature are shown in figure 15 above. Clearly from the figure the ambient temperature and hence the cell temperature negatively affect the efficiencies of the module. The efficiencies were observed to increase when the temperatures decrease and decrease when the temperatures increase. Their correlation coefficients were found as (r = -0.54) and (r = -0.58) for c-Si and mc-Si modules.

All modules show high daily efficiency for low

irradiation. There is correlation between irradiation and module temperature in that when the irradiation increases the temperature of the module increases too at the same time resulting in increased temperature losses (Balaska *et al*, 2017).

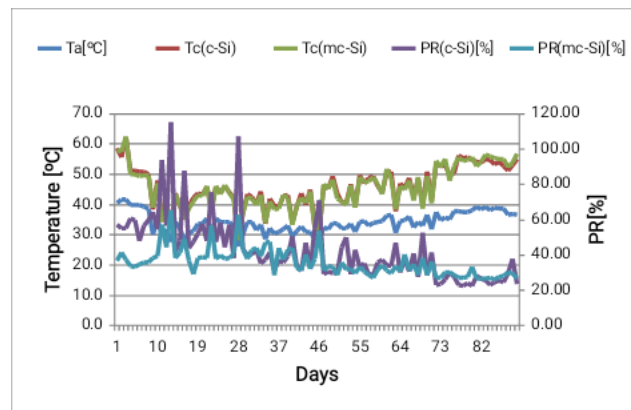


Fig 22. Ambient temperature, cell temperatures and performance ratios over the test period.

The average daily ambient temperature, cell temperature and performance ratio are shown in fig 22. The PR of the modules as expected decreases when the ambient, hence the cell temperature and the daily irradiation increase. This agrees with the work of Aste *et al*, (2014). The correlation coefficient between PR and cell temperature (T_c) in this study was found to be (r = -0.58) for c-Si and (r = -0.70) for mc-Si module. The effects of these cell temperatures on efficiency and performance ratio were shown in fig 23 and 24.

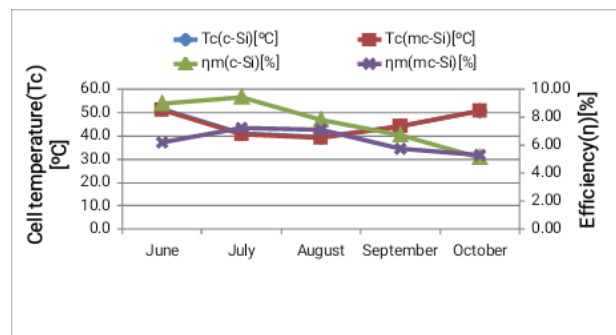


Fig 23. Monthly average daily cell temperatures and monthly efficiency of the modules.

As seen from fig 17 above, the cell temperatures and hence the ambient temperatures negatively affect the efficiencies of the modules. The cell temperatures of c-Si and mc-Si were 51.5°C and 51.1°C in the month of June with corresponding

efficiencies of 8.98% and 6.17%. The cell temperatures decreased to 41.1°C for c-Si and 40.7°C for mc-Si in July and the efficiencies increased to 9.43% and 7.22% respectively. The cell temperatures of c-Si module increased to 44.2°C and 50.6°C in September and October and that of mc-Si module to 43.9°C and 50.8°C accordingly. The corresponding decrease in their efficiencies were 6.67% and 5.11% for c-Si and 5.71% and 5.29% for mc-Si respectively.

The work of Zouui *et al.*, (2015) has shown that for the same irradiance level, the output power and therefore the efficiency decreases with increased cell temperature. The efficiency depends strongly on temperature of the PV module and an overheating causes a decrease in the produced energy.

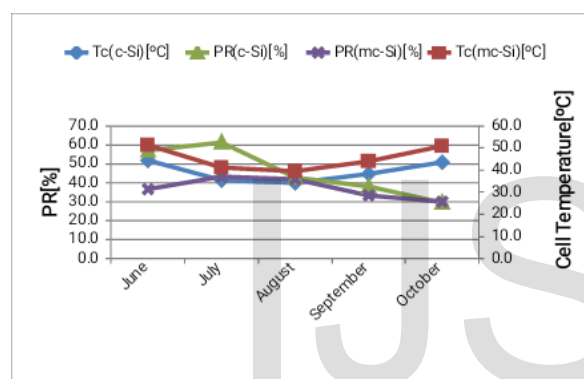


Fig 24. Module temperatures and performance ratios.

From fig 24, the module temperature also affects the performance ratio of the module in the same way it affects efficiency. This is so because the efficiency and the performance ratio are positively correlated as shown in figure 36 and 37. Thus the module temperature affects the efficiency and performance ratio of the PV panel negatively.

4.2.3 Effects of Irradiance on Short-Circuit Current (I_{sc}) and Open-Circuit Voltage (V_{oc}).

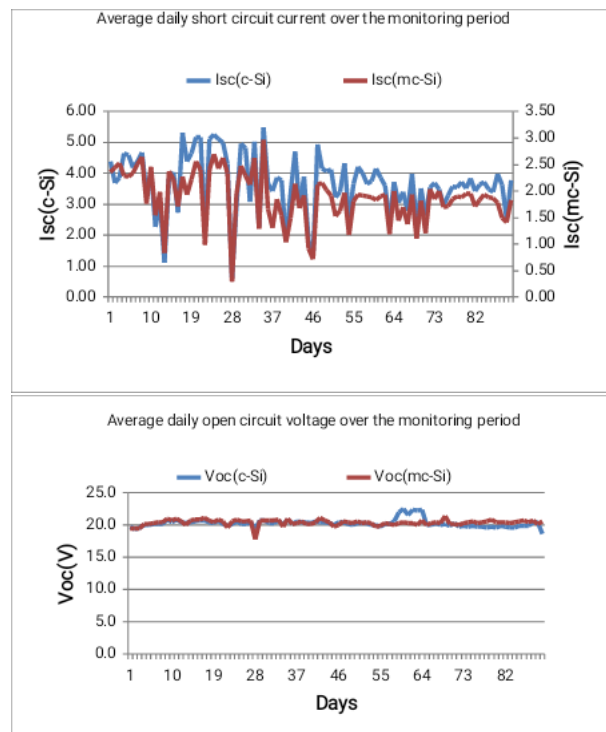


Fig 25. Average daily short circuit current and open circuit voltage during the test period.

Fig 25 shows the short circuit current (I_{sc}) and the open circuit voltage (V_{oc}) over the test period. As seen from the figure, the I_{sc} undergoes several fluctuations but V_{oc} has small fluctuation over the monitored period. This is because I_{sc} is more affected by the irradiation than V_{oc} and this is what Zaoui *et al.*, (2015) also identified. I_{sc} is more positively affected by the irradiation but the temperature negatively affects V_{oc} where the experimental temperature of the cells is higher than 25°C (Zaoui *et al.*, 2015). Figure 26 and 27 below shows the daily irradiance, V_{oc} and I_{sc} over the test period. As explained, the I_{sc} is more effected by the irradiance, the correlation coefficient between G and I_{sc} is ($r = 0.86$) for both modules. The correlation value between the I_{sc} and cell temperature (T_c) is ($r = 0.43$) for c-Si and ($r = 0.45$) for mc-Si module. For correlation coefficient between V_{oc} and T_c the values are ($r = -0.81$) and ($r = -0.42$) respectively. This shows that temperature negatively affects the V_{oc} of c-Si more than that of mc-Si module.

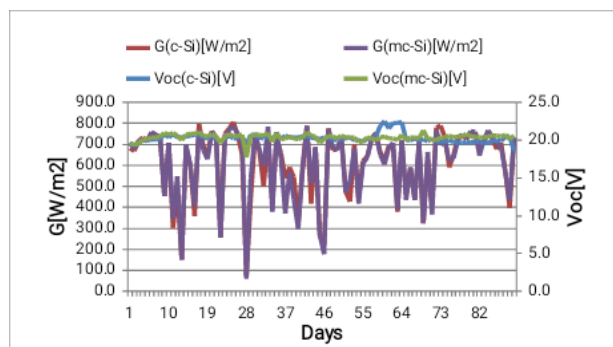


Figure 26. Average daily irradiance and open circuit voltage over the monitoring period.

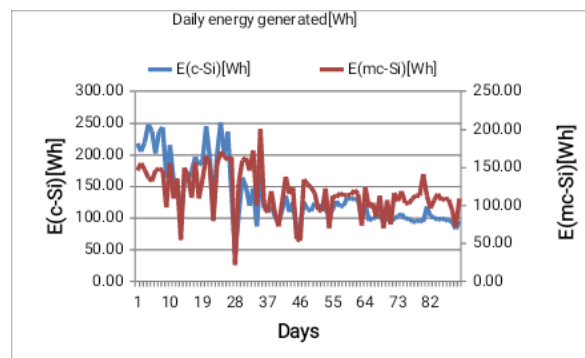


Figure 28. Daily electrical energy generated during the test period.

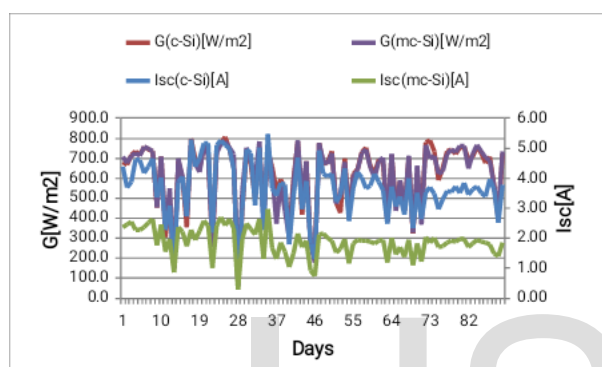


Fig 27. Average daily irradiance and short circuit current over the monitoring period.

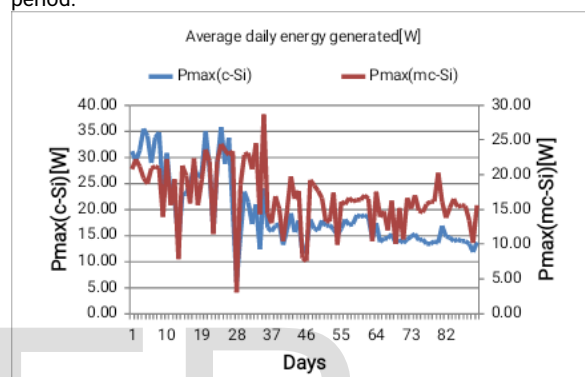


Fig 29. Average daily electrical energy generated during the test period.

4.3 Result of Power Rating Over a Specified Period

Energy yield captures the full picture by measuring energy production in a given location over time (kWh). Energy yield, hence, combines the technological properties of a solar cell with the conditions under which it is operated.

The daily and the average daily energy generated by the modules are shown in figure 28 and 29 below. The generated energy of the modules decreased over time. The maximum produced daily energy was 250.62Wh with an average daily value of 38.80W for c-Si module and 200.33Wh with an average daily value of 28.62W for mc-Si module. Their minimum recorded values were 42.91Wh and 21.24Wh with corresponding averages of 6.13W and 3.03W respectively.

The total electrical energy generated by the monocrystalline (c-Si) and the polycrystalline (mc-Si) modules during the monitoring period was 12096.88Wh (12.10kWh) and 10535.29Wh (10.54kWh) respectively. The monthly average was then 2419.38Wh and 2107.06Wh in that order. Thus monocrystalline module generated more energy than the polycrystalline module.

Figure 30 shows the monthly total and the monthly daily energy generated by the PV systems. Monocrystalline module is characterised by the highest monthly energy production in June, July and September with energy values 2183.66Wh, 2904.20Wh and 2331.80Wh respectively. The energy produced by the polycrystalline module in these months are 1405.45Wh, 2140.69Wh and 2136.64Wh in that respect. However, the polycrystalline module dominates its counterpart in August and October with energy values of 1964.78Wh and 2887.72Wh respectively. The produced energy values of monocrystalline module in these months are 1902.19Wh and 2774.72Wh in that order. Maximum monthly energy production was observed in July and by monocrystalline module.

Elibol *et al.*, (2017) also identified the month of July with highest produced energy and the compared power values of 13.22kWh, 14.16kWh and 14.27kWh were obtained in the month for a-Si, polycrystalline and mono-crystalline panels respectively.

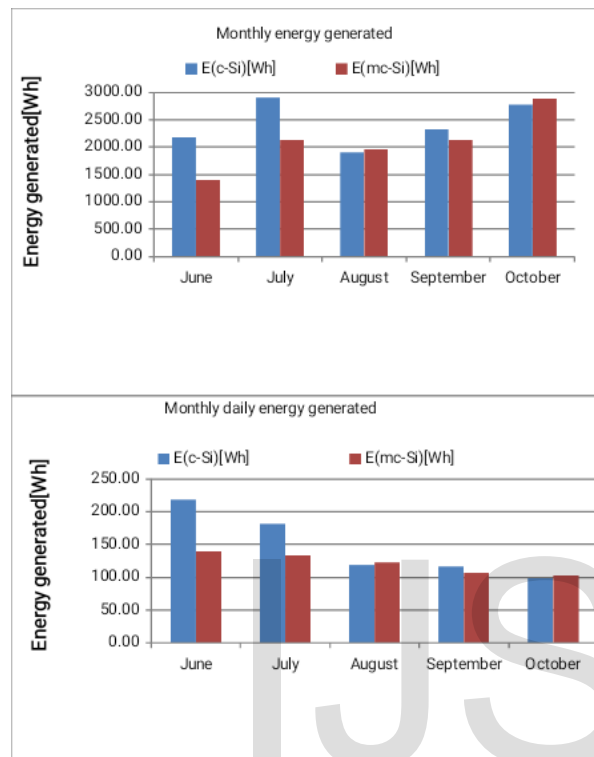


Fig 30. Monthly energy generated and monthly average daily energy generated.

The monthly average energy generated was observed to decrease from June to October. On the average results, the maximum monthly daily energy of 218.37Wh and 140.54Wh were produced in June by mono-crystalline and polycrystalline modules respectively. With respect to monthly daily energy production, June has maximum energy followed by July, August, September and October. This is due to the unequal number of measurement days in the months, and this agrees with the highest monthly average irradiation of 4821.2Wh/m² in the month. The monthly average irradiation in July, August, September and October were 4166.6Wh/m², 3889.0 Wh/m², 4155.2 Wh/m², 4450.6 Wh/m² respectively.

Baharwani *et al.*, (2015) compared polycrystalline and CdTe of same rated power with those used in this study and reported the average energy generated in a day as 225Wh and 132Wh respectively. The monthly average daily energy

generated by the modules are shown in fig 27 below.

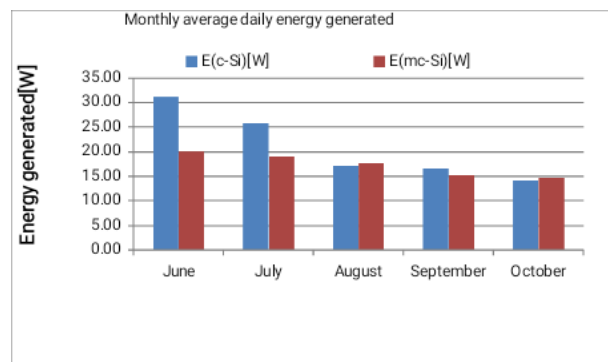


Fig 31. Monthly average daily energy generated.

The monthly average daily energy generated shown in fig 31 represents the hourly values or the Pmax and is obtained by dividing the monthly daily energy with the number of hours (7hours) the modules operate.

According to Bianchini *et al.*, (2016) when the PV modules work in a real environment, the measured DC power (W), P_{DC}, can be very different from the nominal one due to variation in module temperature T_c (°C) and/or irradiance G (W/m²). The paper also highlighted similar experiences carried on in Egypt and showed that even if PV modules are cleaned every day by nonpressurized water, a 50% power decreasing can be measured after 45 days.

In this study we observe a similar scenario and find out the energy generated by the modules in the field to be far below the rated value. The modules were rated on STC and hence their outputs may vary depending on the environmental condition.

The power losses due to the temperature and environmental conditions can become large enough to jeopardize the project success (Tossa *et al.*, 2016).

4.4 Result of Electrical Power Conversion Efficiency (η)

Figure 32 and 33 show daily and monthly the efficiencies of the two modules tested over the monitoring period

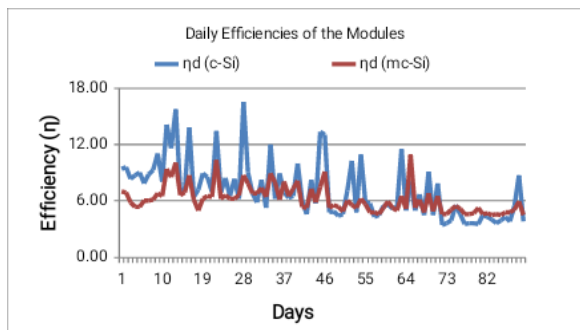


Fig 32. Daily efficiencies of the modules.

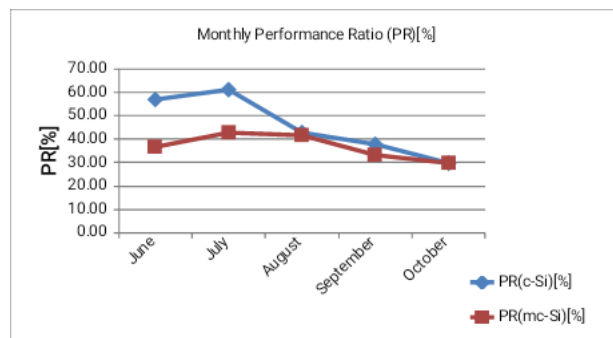


Figure 35. Monthly Performance Ratios of the Modules.

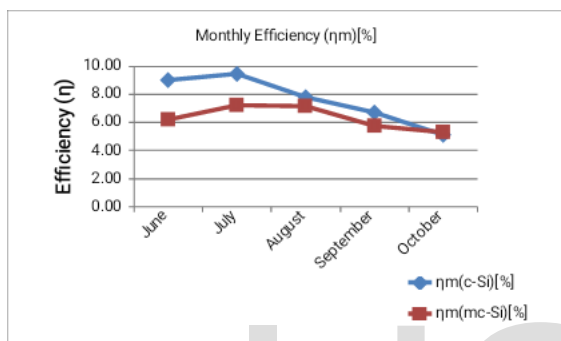


Figure 33. Monthly efficiencies of the modules.

From fig 32-35 the performance ratios and the efficiencies of the the modules follow the same trend as shown in figure 36 and 37 below.

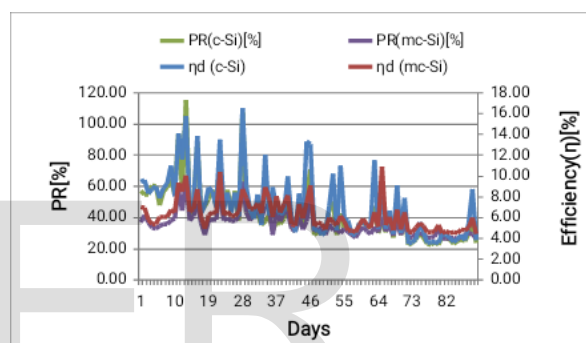


Fig 36. Daily performance ratio (PR) and efficiency during the test period.

4.5 Result of Performance Ratio (PR)

Fig 34 and 35 show the daily and monthly performance ratios of the two modules tested over the monitoring period

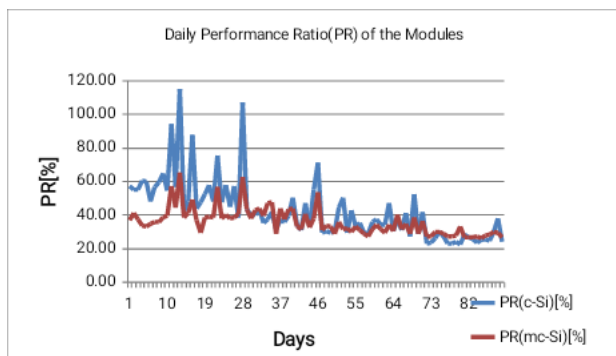


Fig 34. Daily Performance Ratio (PR) of the Modules over the monitoring period.

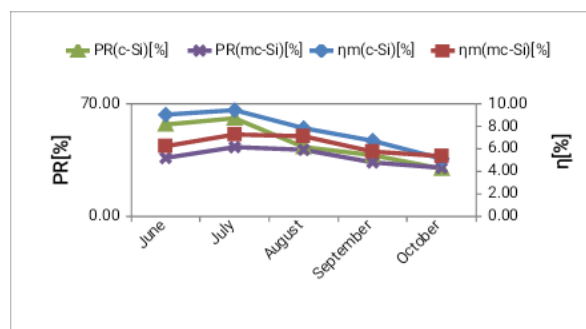


Fig 37. Monthly performance ratios and efficiencies of the modules.

From fig 35 the PR and efficiency are positively related. The highest reached daily PRs were 115.03% and 65.25% by c-Si and mc-Si modules. The minimum recorded values were 22.52% and 26.10% respectively. The correlation coefficients between PR and efficiency were ($r = 0.90$) for c-Si and ($r = 0.91$) for mc-Si module. From fig 36, the performance ratios of the modules in June, July,

August, September and October were 56.92%, 60.80%, 42.62%, 37.76%, 29.40% and 36.39%, 42.78%, 41.46%, 33.13%, 29.72% for the c-Si and the mc-Si modules respectively.

Clearly c-Si module outperforms the mc-Si module in all the months except October. The highest monthly PRs achieved by both modules were 60.80% and 42.78% in July. This correspond with highest efficiencies of 9.43% and 7.22% recorded in the same month respectively. The average performance ratios and efficiencies of the modules across the monitoring period were 45.50%, 36.70% and 7.60%, 6.30% for the c-Si and the mc-Si modules respectively.

Low value of PR usually corresponds to a problem but it may not indicate the typical cause for this behavior. For identifying the actual cause, detailed experiments and analysis have to be carried out. Typical ranges of the PR rose from reportedly 50-75% in the 1980s and 70-80% in the 1990s to > 80% nowadays (Khalid *et al.*, 2016).

Silicon solar cells containing boron and oxygen are one of the most rapidly growing forms of electricity generation. However, they suffer from significant degradation during the initial stages of use. This problem has been studied for 40 years resulting in over 250 research publications (Contreras *et al.*, 2019).

PR is an indicator of losses resulting from inverter problems, wiring, shading, cell mismatch, reflection, outages, module temperatures etc. The temperature of the study environment affects the PR of the modules etc. (Khalid *et al.*, 2016). The temperature of the study environment, cell mismatch and reflection might be the cause of the low PR value observed in this work.

Both the performances and the temperature coefficients given by manufacturers, does not always reflect the modules real performance the sites located in hot climate regions like west Africa (Tossa *et al.*, 2016).

Just of recent Contreras *et al.*, (2019) propose structures of the B_2O_3 defect which match the experimental findings and put forward the hypothesis that the dominant recombination process associated with the degradation is trap-assisted Auger recombination.

In this study, therefore, c-Si module has shown best performance in terms energy generated, efficiency and performance ratio and thus the suitable module for Kebbi State environment.

5.0 Conclusion

This research presents the comparison of two silicon photovoltaic module technology performances under real operating conditions conducted at Bayan Tasha located in Birnin Kebbi, Kebbi State (Nigeria). Performance ratio parameter was chosen in order to compare the PV modules. The I-V characteristics of the modules were measured at regular interval based on the resistive load techniques, during the test period: June, 2018 to October, 2018. The irradiance, ambient and cell temperatures of the modules were also measured. The daily, monthly and the total energy generated over the test period as well as efficiencies and performance ratios were calculated in the excel environment. The outdoor characterization of PV modules is useful for the technologies choice since the modules are rated at the STC which is quite different from the real operating condition. According to the result of this study, the c-Si module outperformed the mc-Si module and hence accepted as best choice for the study environment. The monthly average daily cell temperatures are determined in range of 51.5°C- 39.6°C, with an average of 45.4°C for c-Si and 51.1°C - 39.1°C, with an average of 45.1°C for mc-Si. The average daily irradiation is found in the range of 668.7W/m²-560.4 W/m², with an average of 614.8 W/m² for c-Si and for mc-Si as 692.0W/m²-557.1W/m², with an average of 615.1W/m² respectively. The average ambient temperature over the monitoring period was found as 34.2°C.

A positive correlation was observed between, irradiance and ambient temperature, module temperature and the ambient temperature, the PR and efficiency.

The ambient temperature and hence the cell temperature negatively affect the efficiencies and thus the PRs of the modules. The correlation coefficients between T_c and η were found as ($r = -0.54$) and ($r = -0.58$) for c-Si and mc-Si modules, thus mc-Si is slightly more affected by the temperatures.

The I_{sc} and irradiance were positively correlated and the correlation coefficient between them is ($r = 0.86$) for both modules. The irradiance was observed to have a less effect on V_{oc} . I_{sc} was observed to undergo several fluctuations but V_{oc} has small fluctuation over the monitored period and this is because I_{sc} is more affected by the irradiation than V_{oc} .

The correlation value between the I_{sc} and cell temperature (T_c) is ($r = 0.43$) for c-Si and ($r = 0.45$) for mc-Si module. For correlation coefficient between V_{oc} and T_c the values are ($r = -0.81$) and ($r = -0.42$) respectively. This shows that temperature

positively affects I_{sc} and negatively affects the Voc. It affects Voc of c-Si more than that of mc-Si module.

The total electrical energy produced over the monitoring period was 12.10kWh and 10.54kWh with an average of 2.42kWh and 2.11kWh for c-Si and mc-Si modules respectively.

The performance ratios and the efficiencies of the modules were observed to follow the same trend. The efficiencies of the modules were found to be 7.60% and 6.30% and the performance ratios as 45.50% and 36.70% in the same order. The polycrystalline module as observed to outperformed the monocrystalline module in terms of energy in the months of August and October, and in terms of performance ratio in the month of October.

In conclusion the findings of this study show the c-Si module as the best choice in terms energy generated, efficiency and performance ratio and thus the suitable module for Kebbi State environment.

Observations developed in this study can be used for the selection of the most suitable PV technology, depending on the climatic conditions.

-
- *Abubakar Ohinoyi Musa is a professor of physics at Bayero University Kano, P.M.B.3011, Kano, Nigeria. E-mail: aomusa.phy@buk.edu.ng.*
 - *Adamu Bala Isah is currently pursuing masters degree program in physics at Bayero University Kano, P.M.B.3011, Kano, Nigeria, E-mail: isahdamu@mail.com.*

References

- Almonacid, F., Fernandez, E. F., Mellit, A., & Kalogirou, S. (2016). Review of techniques based on artificial neural networks for the electrical characterization of concentrator photovoltaic technology. *Renewable and Sustainable Energy Reviews*, (October), 0–1. <https://doi.org/10.1016/j.rser.2016.11.075>
- Aste, N., Del Pero, C., & Leonforte, F. (2014). PV technologies performance comparison in temperate climates. *Solar Energy* 109, 1–10, <http://dx.doi.org/10.1016/j.solener.2014.08.015>.
- Baharwani, V., Meena, N., Sharma, A., Stephen, R. B., Mohanty, P. (2015). Comparative Performance Assessment of different Solar PV Module Technologies. *International journal of innovations in Engineering and Technology (IJJET)*, 5(1), ISSN: 2319-1058.
- Balaska, A., Tahri, A., Tahri, F., & Stambouli, A. B. (2017). Performance assessment of five different photovoltaic module technologies

under outdoor conditions in Algeria. *Renewable Energy*.

- <https://doi.org/10.1016/j.renene.2017.01.057>
- Başoğlu, M.E., Kazdaloğlu, A., Erfidan, T., Bilgin, M.Z., & Çakır, B. (2015). Performance analyzes of different photovoltaic module technologies under İzmit, Kocaeli climatic conditions. *Renewable and Sustainable Energy Reviews* 52, 357–365, <http://dx.doi.org/10.1016/j.rser.2015.07.108>.
- Berwal, A. K., Kumar, S., Kumari, N., Kumar, V., & Haleem, A. (2017). Design and analysis of rooftop grid tied 50 kW capacity Solar Photovoltaic. *Renewable and Sustainable Energy Reviews*, (March), 1–11. <https://doi.org/10.1016/j.rser.2017.03.017>
- Bianchini, A., Gambuti, M., Pellegrini, M., Saccani, C. (2016). Performance analysis and economic assessment of different photovoltaic technologies based on experimental measurements. *Renewable Energy* 85 (2016) 1-11 <http://dx.doi.org/10.1016/j.renene.2015.06.017>.
- Carr, A.J., & Pryor, T.L. (2004). A comparison of the performance of different PV module types in temperate climates. *Solar Energy*, (January), 76, 285-294. <https://doi.org/10.1016/j.solener.2003.07.026>
- Chandel, S. S., & Agarwal, T. (2017). Review of cooling techniques using phase change materials for enhancing efficiency of photovoltaic power systems. *Renewable and Sustainable Energy Reviews*, 73 (October), 1342–1351. <https://doi.org/10.1016/j.rser.2017.02.001>
- Commission, E. (2009). Photovoltaic Solar Energy; Development and Current Research. Luxemburg; Office for Official Publications of the European Union. <https://doi.org/10.2768/38305>.
- Contreras, M.V., Markevich, V.P., Coutinho, J., Santos, P., Crowe, I.F., Halsall, M.P., Hawkins, ... Peaker, A.R. (2019). Identification of the mechanism responsible for the boron oxygen light induced degradation in silicon photovoltaic cells *Journal of Applied Physics (J. App. Phys)*. 125, 185704 (2019), <https://doi.org/10.1063/1.5091759>.
- Elibol, E., Özmen, Ö.T., Tutkun, N., & Köysal, O. (2017). Outdoor performance analysis of different PV panel types. *Renewable and Sustainable Energy Reviews* 67, 651–661, <http://dx.doi.org/10.1016/j.rser.2016.09.051>.
- Ellabban, O., Abu-rub, H., & Blaabjerg, F. (2014).

- Renewable energy resources : Current status , future prospects and their enabling technology. *Renewable and Sustainable Energy Reviews*, 39, 748–764. <https://doi.org/10.1016/j.rser.2014.07.113>
- Espinosa, N., Abad, J., & Urbina, A. (2017). The greenest decision on photovoltaic system allocation, 101, 1348–1356. <https://doi.org/10.1016/j.renene.2016.10.020>
- Fesharaki, V. J., Dehghani, M., & Fesharaki, J. J. (2011). The Effect of Temperature on Photovoltaic Cell Efficiency, (November), 20–21.
- Garoudja, E., Harrou, F., Sun, Y., Kara, K., Chouder, A., & Silvestre, S. (2017). Statistical fault detection in photovoltaic systems. *Solar Energy*, 150, 485–499. <https://doi.org/10.1016/j.solener.2017.04.043>
- Green, M. A. (1982). *Solar Cells: Operating Principle: Technology and System Applications*. <https://doi.org/10.1063/1.4922493>
- Grid, S. (2010). Critical Factors that Affecting Efficiency of Solar, 2010(May), 47–50. <https://doi.org/10.4236/sgre.2010.11007>
- Guwaeder, A., & Ramakumar, R. (2017). A Study of Grid-connected Photovoltaics in the Libyan Power System, 7(2), 41–49. <https://doi.org/10.5923/j.ep.20170702.02>
- Islam, M. M., Pandey, A. K., Hasanuzzaman, M., & Rahim, N. A. (2016). Recent progresses and achievements in photovoltaic-phase change material technology : A review with special treatment on photovoltaic thermal-phase change material systems. *Energy Conversion and Management*, 126, 177–204. <https://doi.org/10.1016/j.enconman.2016.07.075>
- Ismail, A. & Oke I.A. (2012). Trend analysis of precipitation in Birnin Kebbi, Nigeria. *International Research Journal of Agricultural Science and Soil Science* (ISSN: 2251-0044) 2(7) pp. 286-297, <http://www.interestjournals.org/IRJAS>.
- Jäger, K., Isabella, O., Smets, A.H.M., René, A.C.M.M., Swaaij, V., and Zeman, M. (2014). "Solar Energy Fundamentals, Technology, and Systems." 2014. Delft University of Technology; edX.
- Ju, X., Xu, C., Han, X., Du, X., Wei, G., & Yang, Y. (2017). A review of the concentrated photovoltaic / thermal (CPVT) hybrid solar systems based on the spectral beam splitting technology. *Applied Energy*, 187, 534–563. <https://doi.org/10.1016/j.apenergy.2016.11.087>
- Khalid, A.M., Mitra, I., Warmuth, W., & Schacht, V. (2016). Performance ratio – Crucial parameter for grid connected PV plants. *Renewable and Sustainable Energy Reviews* 65 (2016) 1139–1158, <http://dx.doi.org/10.1016/j.rser.2016.07.066>.
- Krauta, S. (2006). *Solar Electric Power Generation; Photovoltaic Energy Systems; Modeling of Optical and Thermal Performance, Electrical Yields, Energy Balance, Effect on Reduction of Greenhouse Gas Emissions*. Berlin Heidelberg; Springer.
- Kumar, M., & Kumar, A. (2017). Performance assessment and degradation analysis of solar photovoltaic technologies : A review. *Renewable and Sustainable Energy Reviews*, 78(March), 554–587. <https://doi.org/10.1016/j.rser.2017.04.083>
- Mathew, M., Kumar, N.M., Koroth, R.P. (2018). Outdoor measurement of mono and poly c-Si PV modules and array characteristics under varying load in hot-humid tropical climate. *Materials Today: Proceedings* 5 (2018) 3456–3464. www.materialstoday.com/proceedings.
- Musa, A.O. (2010). *Principles of Photovoltaic energy Conversion*. Zaria (Nigeria); Ahmadu Bello University Press Limited.
- Ogunbajo, R.A., Ajayi, M.T.A., Usman B.S. & Wali, R. (2015). Spatial variations in residential property development in Birnin Kebbi, Nigeria. *Ethiopian Journal of Environmental Studies & Management* 8(2): 206 – 224, doi: <http://dx.doi.org/10.4314/ejesm.v8i2.10>.
- Pagliari, M., Palmisano, G., and Ciriminna, R. (2008). Chemistry & biodiversity *Flexible Solar Cells-- Book*. <http://onlinelibrary.wiley.com/doi/10.1002/cbdv.200490137/abstract>.
- Peters, I.M., Liu, H., Reindl, T., & Buonassisi, T., (2018). Global Prediction of Photovoltaic Field Performance Differences Using Open-Source Satellite Data. *Joule* 2, 307–322 (February) Elsevier Inc. <https://doi.org/10.1016/j.joule.2017.11.012>
- Polo, J., Alonso-abella, M., Ruiz-arias, J. A., & Balenzategui, J. L. (2017). Worldwide analysis of spectral factors for seven photovoltaic technologies, 142, 194–203. <https://doi.org/10.1016/j.solener.2016.12.024>
- Rao, S. & Parulekar, B.B. (2007). *Energy*

Technology; Nonconventional, Renewable & Conventional.

3rd Edn., Nai Sarak, Delhi; Romesh Chander Khanna for KHANNA PUBLISHERS.

Reza, M., Hizam, H., Gomes, C., Amran, M., Ismael, M., & Hajighorbani, S. (2016). Power loss due to soiling on solar panel: A review. *Renewable and Sustainable Energy Reviews*, 59, 1307–1316.

<https://doi.org/10.1016/j.rser.2016.01.044>

Rode, J., & Weber, A. (2016). Does localized imitation drive technology adoption? A case study on rooftop photovoltaic systems in Germany. *Journal of Environmental Economics and Management*, 78, 38–48. <https://doi.org/10.1016/j.jeem.2016.02.001>

Sathe, T. M., & Dhoble, A. S. (2017). A review on recent advancements in photovoltaic thermal techniques. *Renewable and Sustainable Energy Reviews*, 76(October 2016), 645–672. <https://doi.org/10.1016/j.rser.2017.03.075>

Sharma, S., Jain, K. K., & Sharma, A. (2015). Solar Cells: In Research and Applications – A Review, (December), 1145–1155.

Shukla, A. K., Sudhakar, K., & Baredar, P. (2016). Simulation and performance analysis of 110 kW p grid-connected photovoltaic system for residential building in India: A comparative analysis of various PV technology. *Energy Reports*, 2, 82–88. <https://doi.org/10.1016/j.egypr.2016.04.001>

Siddiqui, R., Kumar, R., Jha, G. K., Gowri, G., Morampudi, M., Rajput, P., ... Nanda, G. (2016). Comparison of different technologies for solar PV (Photovoltaic) outdoor

performance using indoor accelerated aging tests for long term reliability. *Energy*, 107, 550–561.

<https://doi.org/10.1016/j.energy.2016.04.054>
Singh, G. K. (2013). Solar power generation by PV (photovoltaic) technology : A review. *Energy*, 53, 1–13.

<https://doi.org/10.1016/j.energy.2013.02.057>
Tossa, Alain K et al. 2016. "Energy Performance of Different Silicon Photovoltaic Technologies under Hot and Harsh Climate." *Energy* 103: 261–70.

<http://dx.doi.org/10.1016/j.energy.2016.02.133>.

Sommerfeld, J., Buys, L., Mengersen, K., & Vine, D. (2017). Influence of demographic variables on uptake of domestic solar photovoltaic technology. *Renewable and Sustainable*

Energy Reviews, 67, 315–323.

<https://doi.org/10.1016/j.rser.2016.09.009>

Waheed, A., Ahmed, A., & Zahedi, G. (2012). Greener energy: Issues and challenges for Pakistan – Solar energy prospective. *Renewable and Sustainable Energy Reviews*, 16(5), 2762–2780.

<https://doi.org/10.1016/j.rser.2012.02.043>

Zaoui, F., Titaouine, A., Becherif, M., Emziane, M., & Aboubou, A. (2015). A combined experimental and simulation study on the effects of irradiance and temperature on photovoltaic modules. *Energy Procedia* 75 (2015) 373 – 380, <https://doi.org/10.1016/j.egypro.2015.07.393>.